Korean J. Chem. Eng., **29**(12), 1695-1699 (2012)
DOI: 10.1007/s11814-012-0079-z

Effect of acid type in WO_X clusters on the esterification of ethanol with acetic acid

Jae Ryul Park, Byoung Kyu Kwak, Dae Sung Park, Tae Yong Kim, Yang Sik Yun, and Jongheop Yi†

World Class University (WCU) Program of Chemical Convergence for Energy & Environment (C2E2),
School of Chemical and Biological Engineering, Institute of Chemical Process,
Seoul National University, Seoul 151-744, Korea
(*Received 19 January 2012 • accepted 25 May 2012*)

Abstract−Tungsten oxide clusters supported on silica (WO_X/SiO_2) with different W loading levels and the effect of acid type on the esterification of acetic acid with ethanol were examined. The catalysts were characterized using various techniques (XRD, Raman spectroscopy, NH_3-TPD and FT-IR) to investigate the crystallinity and the nature of the acid sites. The change in the composition of two tungsten oxide species (polytungstate and crystalline WO_3) leads to the change of Lewis acid to Brønsted acid ratio. Importantly, the ratio of the two different acid types has a substantial effect on the catalytic activity. The fraction of Lewis acid to total acid sites rapidly changed from 23% to 77% due to the presence of crystalline WO_3. Where the Lewis acid sites accounted for 55% of the total acid sites, the WO_X/SiO_2 catalyst showed the highest catalytic activity among the prepared catalysts.

Key words: Esterification, Tungsten Oxide, WO_X/SiO_2, Ethyl Acetate

INTRODUCTION

Esterification has the potential for the production of value-added chemicals from alcohols and organic acids. Ethyl acetate, the product of the esterification of ethanol with acetic acid, is widely used in perfumes, solvents, paint products and pharmaceuticals [1,2]. The conventional esterification process involves the use of acidic catalysts, such as H_2SO_4 and HF in homogeneous solution [3,4]. Although the catalytic activity of these acid catalysts is high, there are significant drawbacks, including product separation and reactor corrosion problems [5]. Therefore, considerable efforts have been made to develop heterogeneous catalysts for the esterification, in order to overcome these problems [2-4]. It is generally known that acid sites are the active sites for esterification. Shanks et al. [7] prepared surface-modified SBA-15 for the esterification of acetic acid with methanol in an attempt to better understand the esterification reaction. Wu et al. [7] reported on the gas-phase esterification of acetic acid with ethanol using silicotungstic acid catalyst supported on the activated carbon.

Supported tungsten oxide is a highly acidic metal oxide that contains both Lewis and Brønsted acid sites and has been widely used as an acid catalyst in dehydration and cracking reactions. Various supports have been used for this catalyst, including ZrO_2, TiO_2, etc [9,10]. There are two types of tungsten oxide structures on supports, and their composition is dependent on the weight of tungsten that is loaded on the support [9]. One form is crystalline WO_3, which has a distorted octahedral structure showing Lewis acid properties corresponding to the unsaturated W^{6+} species in crystalline WO_3 [9]. This species has the ability to interact with both alcohols and acids via interactions between unpaired electrons in organic molecules and water with Lewis acid sites on crystalline WO_3 [11,12]. The other is a polytungstate forming keggin-structure, which has both Lewis acid and Brønsted acid properties, corresponding to a Si-O-W bridge site and a terminal W=O structure, respectively [9]. Polytungstate species on silica showed a high activity because it is similar to the structure of silicotungstic acid, which is a highly effective catalyst for esterification reactions. When the tungsten loading is low, polytungstate is mainly present in the form of WO_X clusters, but crystalline WO_3 begins to form rapidly as the amount of tungsten loading is increased [13]. In previous studies, it has been claimed that an ensemble effect of polytungstate and crystalline WO_3 improved the acidity of catalysts when the appropriate amount of tungsten was loaded on the support [9]. The optimum loading level was determined according to the reactions such as dehydration and isomerization. However, the improvement in acidity was imperceptible and a valid explanation for this high activity remains unexplained.

In this study, we investigated the use of tungsten oxide catalyst supported on silica for the esterification of acetic acid with ethanol and determined the optimum loading level of tungsten for target reaction. The characteristics of the prepared catalysts, along with other influential factors, were examined via characterization and quantitative analysis.

EXPERIMENTAL

1. Catalyst Preparation

The WO_X/SiO_2 samples were prepared with different tungsten loadings by an incipient wetness impregnation method. The precursors were used for preparing aqueous solutions containing known amounts of ammonium metatungstate ($(NH_4)_6H_2W_{12}O_{40}\cdot xH_2O$, Sigma Aldrich). The impregnated catalysts were dried overnight in an oven at 80 °C for overnight under air condition, and then calcined at 450 °C for 4 h in atmosphere of air. Aerosil 200 (SiO_2), as the silica support, with specific surface area of 200 $m^2\ g^{-1}$ was obtained from Degussa. The prepared samples were denoted by their weight percentage of

†To whom correspondence should be addressed.
E-mail: jyi@snu.ac.kr

W. For example, 3WS indicates a catalyst containing 3 wt% tungsten supported on the silica support.

2. Catalyst Characterization

X-ray diffraction (XRD) was used to determine the crystallinity of the catalysts using D-MAX2500-PC (Rigaku Corp.) with CuKα radiation (λ=1.5405 Å) in an operating mode of 50 kV and 100 mV. XRD data were recorded from 10°-80° in a step of 10° min^{-1}. Raman spectra in the 600-1,000 cm^{-1} range were recorded on a Jobin Ynon spectrometer, model T64000, using a 514 nm Ar laser as an exciting source. The NH_3-TPD was carried out to measure the quantity of acid sites on the catalyst. Before the measurements, all samples were pretreated in a stream of helium at 400 °C for 4 hr. After cooling to 50 °C, a mixture of ammonia/helium (5 vol% ammonia) was allowed to flow through sample for 1 hr. Physically adsorbed ammonia was removed by increasing the temperature of the helium flow to 100 °C for 20 min. The temperature was then increased linearly at a ramping rate of 10 °C min^{-1} up to 400 °C. The desorbed ammonia was measured by means of a thermal conductivity detector (TCD). IR spectra were recorded with a M2000 instrument (MIDAC corp.) An FT-IR spectrophotometer, with a quartz cell to hold samples was used to collect FT-IR data. The 40 mg of catalysts were pelletized to thin disks which were calcined at 250 °C in He atmosphere for 2 hr to remove water from the samples. The adsorption of ammonia was carried out at room temperature, followed by evacuation to remove physically adsorbed ammonia at the same temperature. FT-IR spectra were also recorded in a vacuum system at room temperature.

3. Catalytic Activity Test

The catalytic activities for the esterification of acetic acid with ethanol were evaluated using a high-pressure continuous reactor (HPCR) in which the reactants were held in the liquid phase, while the actual temperature exceeded the boiling point of the reactants. In previous studies, a semi-batch reactor with a condenser, a batch reactor and a gas-phase reactor were used for this reaction [6,14,15]. However, there were some problems such as limitations in the operating temperature, non-continuous system and coke deposition at high temperature. We developed a new system, a high-pressure continuous reactor (HPCR), which overcomes several problems associated with previous reactor systems. The reactant was prepared by mixing ethanol with acetic acid in 2 to 1 molar ratio. The reaction was performed with 0.3 g catalyst in a fixed bed steel reactor at 160 °C and the pressure was maintained at 3 MPa to maintain the reactant in the liquid phase. The prepared reactant solution was injected into the system at a rate of 0.3 ml min^{-1} by a high pressure pump. After the reaction was complete, the product was cooled by a cooling trap and the reaction products collected in a sampling pot. The product was analyzed by gas chromatography (GC DS 6200, DONAM INSTRUMENT INC.) equipped with a flame ionization detector (FID) and a capillary column (DB-WAX , 30 m×320 μm×0.5 μm).

RESULTS AND DISCUSSION

1. Catalytic Performance for the Esterification of Ethanol with Acetic Acid

The result of the catalytic performance for esterification of acetic acid with ethanol on the WO_X/SiO_2 catalysts is shown in Fig. 1. The selectivity for ethanol esterification was almost 100%, as has been

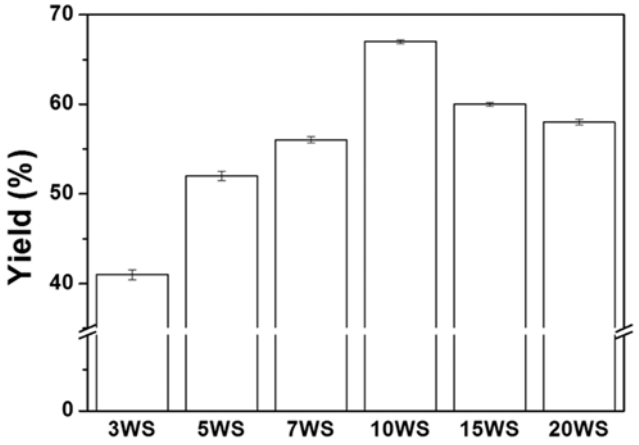

Fig. 1. Catalytic activity of various loading levels of tungsten oxide catalyst (reaction conditions: 160 °C and 36 bar).

verified in previous studies [8]. In the range of 3WS to 10WS, the catalytic activity accelerated with increasing loading levels. The 10WS catalyst resulted in the highest yield of ethyl acetate of about 68% among the prepared catalysts tested. In the case of higher loadings of tungsten, i.e., 15WS and 20WS, the yield of ethyl acetate slowly decreased to around 60%. The curve for catalytic activity was volcano-shaped as a function of loading weight. Because of this, further investigations were conducted to identify the properties of prepared catalysts and relationships between catalyst characteristics and activity for the esterification reaction.

2. Characterization of Tungsten Oxide Catalysts Supported on Silica

XRD analyses were conducted to evaluate the crystallinity of the catalysts. XRD patterns of the WO_X/SiO_2 samples with various tungsten loadings are shown in Fig. 2. Crystalline WO_3 is formed by the thermal decomposition of ammonium metatungstate used as a precursor [9,16,17]. According to PDF# 321395 in JCPDS data

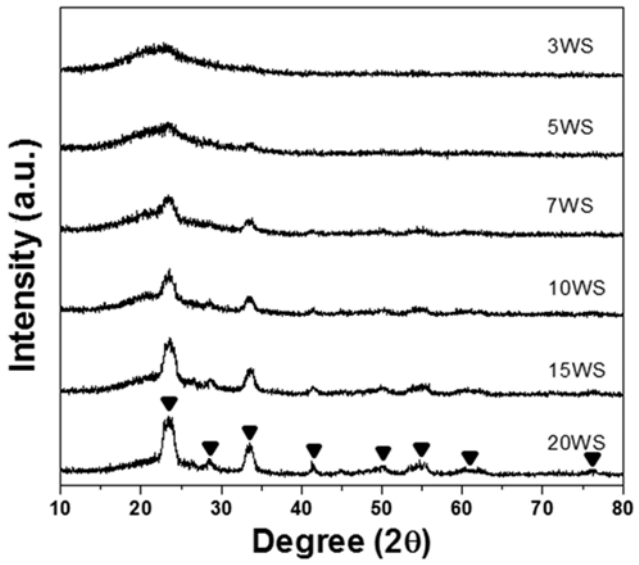

Fig. 2. XRD patterns of WO_X/SiO_2 catalyst with various amounts of loaded W (▼: WO_3).

and previous studies, typical peaks for crystalline WO_3 are found at ca. 23.7°, 29.0°, 33.6°, 41.9° and other peaks over 40° [18]. In the 3WS and 5WS samples, an amorphous phase was observed, i.e., only a broad peak corresponding to silica was observed at 23°. This indicates that the tungsten oxide was highly dispersed on the surface of the silica in the samples because of the low loading amounts used. In the case of 7WS, only a few characteristic peaks for crystalline WO_3 peaks were clearly seen at around 24° and 34° with a weak intensity in the XRD patterns. Also, when the loading amount of W was increased, the amount of crystalline WO_3 in the catalyst was increased, and the 20WS sample showed the highest WO_3 crystallinity. Amorphous polytungstate with Brønsted acid sites is formed when the amount of loaded tungsten is low. Meanwhile, crystalline WO_3 was formed at high loadings and the amount crystalline WO_3 increased with increasing loading.

Raman spectroscopy was used to confirm the crystallinity of catalysts on surface [18]. Characteristic peaks of crystalline WO_3 appeared at 804 cm^{-1} and 720 cm^{-1} corresponding to W-O stretching and bending vibrations, respectively [19]. The characteristic peak for polytungstate was faintly observed at 980 cm^{-1} [12], but it has been reported that this peak is too weak to permit accurate calculations to be made [20]. All peak spectra were tilted slightly, because of the fluorescence of tungsten.

The Raman spectra shown in Fig. 3 were in good agreement with the XRD results. In Raman spectra, peaks corresponding to WO_3 were not observed among samples 3 to 7WS. Small peaks at 804 and 702 cm^{-1} appeared in the case of 10WS, and the size of the peaks increased with increased loading. This suggests that the amount of crystalline WO_3 at the surface was increased. The sensitivity of XRD was similar to that for Raman spectroscopy in a previous study, and is in good agreement with our result of XRD and Raman spectra [21]. When the weight of tungsten loading exceeded 10 wt%, a peak assigned to the vibration of crystalline WO_3 was observed in the Raman spectra. From this result, the surface crystallinity of the prepared catalysts also increased with increasing amounts of tungsten oxide loading.

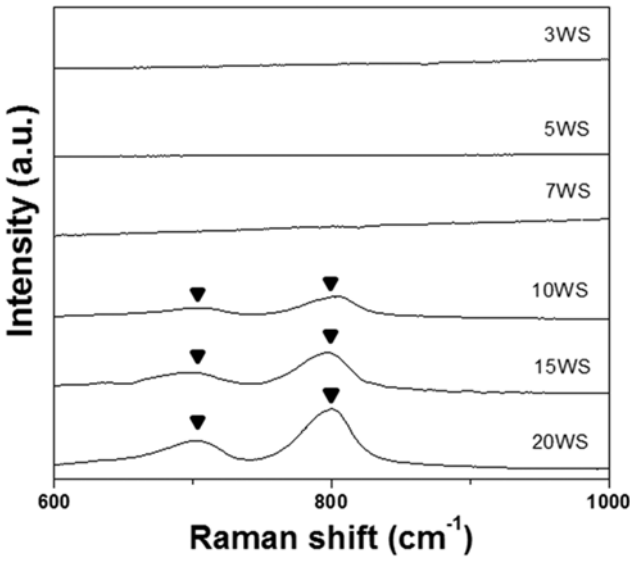

Fig. 3. Raman spectra of WO_X/SiO_2 catalysts with different W loading (▼: crystalline WO_3).

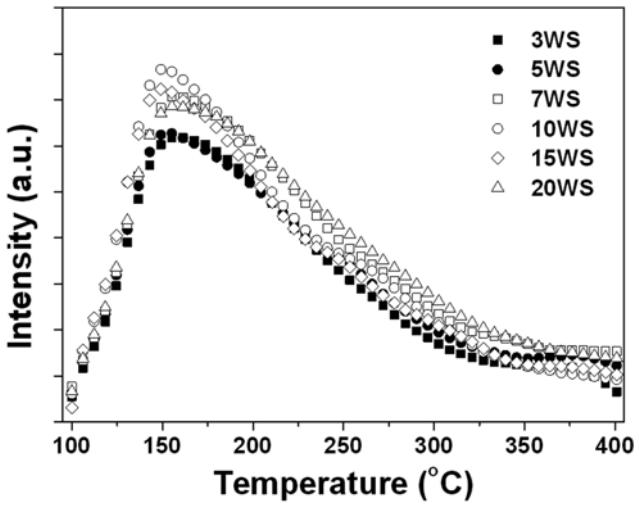

Fig. 4. NH_3-TPD profile of the WO_X/SiO_2 catalysts up to 400 °C.

Ammonia temperature-programmed desorption (NH_3-TPD) experiments were performed to measure the quantity and strength of the acidic sites, as shown in Fig. 4. The ammonia desorption peak was observed at ~150 °C with broad shoulder about 350 °C [15]. In the cases of 3WS and 5WS, a small desorption peak appeared compared to the other catalysts due to the relatively less amount of acid sites, 0.132 mmol/g and 0.143 mmol/g, respectively. This suggests that the low catalytic activities of 3WS and 5WS were due to the small amounts of active sites, because it has been previously established that the number of acid sites is a crucial factor in such esterification reactions [7]. For 7WS, 10WS, 15WS, and 20WS in Fig. 4, TPD profiles had the subequal peak position and similar peak area at all temperatures, and significant improvement in acidity was rarely found. Their acid amounts are 0.172, 0.164, 0.156, 0.176 mmol/g, respectively. They did not exhibit any relationship between activities. From this result, we conclude that the main factor that affects catalytic activity is not only the amount of acid sites, but also other properties of the catalysts. For this reason, further studies regarding the specific acid properties of prepared catalyst were pursued to identify other factors that may affect ethanol esterification.

IR spectroscopy of NH_3 as a probe molecule was conducted to identify the nature of the acid sites (Lewis acid and Brønsted acid) on the surface of catalysts. The spectra of NH_3 adsorbed on catalysts after outgassing at room temperature are shown in Fig. 5. Adsorption bands at 1,618 and 1,458 cm^{-1}, corresponding to Lewis and Brønsted acid sites respectively, were observed in FT-IR spectra [22]. Crystalline WO_3 and part of the polytungstate corresponding to Lewis acid site accounted for adsorption band at 1,618 cm^{-1} due to the asymmetric bending vibration of ammonia adsorbed to Lewis acid sites [23]. A part of the polytungstate contributed to a band at 1,450 cm^{-1} due to ammonium ion (NH_4^+) on Brønsted acid site [23].

Peaks corresponding to the two acid types were observed in all of the prepared catalysts, indicating that both Lewis and Brønsted acid sites are present on the catalysts. Table 1 shows the integrated intensities of bands caused by adsorbed ammonia, and the fraction of Lewis acid to total acid sites was calculated from the adsorption coefficient of NH_3. The ratio of the adsorption coefficient was applied

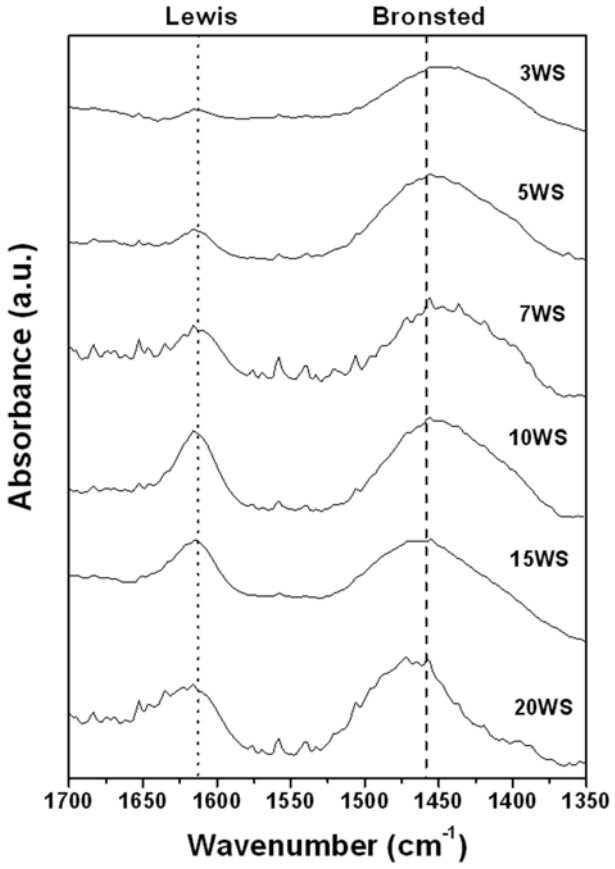

Fig. 5. FT-IR spectra of NH_3 adsorbed on various loading levels of tungsten catalyst (WO_X/SiO_2) at 25 °C.

Table 1. Integrated infrared absorbance for ammonia on prepared catalysts

	3WS	5WS	7WS	10WS	15WS	20WS
L acid site	0.735	1.02	1.01	2.27	3.02	2.33
B acid site	2.43	2.23	1.15	1.85	1.55	0.68
L/(B+L)	0.23	0.32	0.47	0.55	0.66	0.77

*The ratio of the adsorption coefficient (R) is 7, $R=\in^{+}_{NH_4}/\in_{NH_3}$)

to calibrate the gap in the affinity of NH_3 to Lewis and Brønsted acid [24]. The fraction of Lewis acid sites to total acid sites (L/(B+L)) increased with increasing amounts of tungsten oxide on the support. This is due to the crystalline WO_3 which was easily formed in high loading samples corresponding to Lewis acids. These findings are in good agreement with the XRD and Raman spectroscopy data. Although the number of acid sites of catalysts containing over 7 wt% tungsten was almost the same from the NH_3-TPD results, the fraction of Lewis acid sites shown in Table 1 was clearly different for the prepared catalysts. In the case of 7WS, the portion of Lewis acid sites was only 47%; however, 77% of the total acid sites in 20WS were Lewis acid sites. In a previous study, the role of two acid sites was reported to be different [25,26]. A Brønsted acid site can act as the main active site in alcohol esterification, and the Lewis acid site can draw the reactant due to interaction between the Lewis acid site and unpaired electrons in reactants such as alcohol and acetic acid.

The correlation between the fraction of Lewis acid sites to total

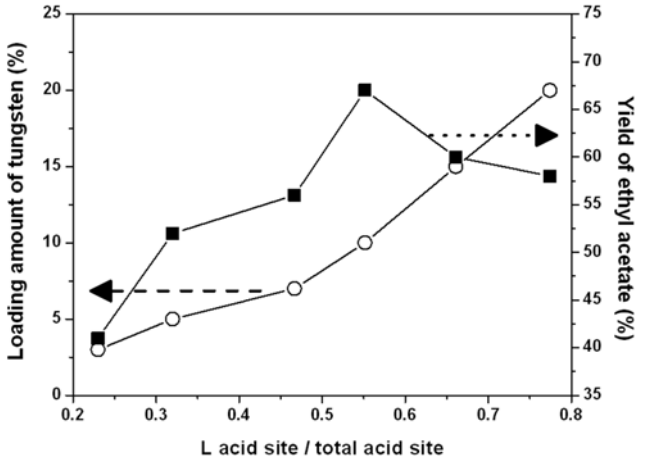

Fig. 6. Catalytic activity of WO_X/SiO_2 as a function of the Lewis acid sites fraction.

acid sites and the yield of ethyl acetate is shown in Fig. 6. In range of 23% to 77% of the portion of Lewis acid sites, the yield of ethyl acetate exhibited a volcano-shaped curve and the optimum value the esterification was around 55%. Even though total acid amounts were almost same for the catalysts containing over 7 wt% of tungsten, the 7WS sample exhibited a low catalytic activity because of the relatively small amount of Lewis acid site. In contrast, the performance of the 15WS and 20WS samples was low, due to a shortage of Brønsted acid sites which are the main active site for esterification.

When tungsten oxide catalyst supported on Areosil 200 was prepared by the incipient impregnation method with various loading levels, catalytic activity showed a volcano-shaped curve. Among the 3WS to 20WS samples, 3WS and 5WS has a small amount of acid sites, as evidenced by the NH_3-TPD profiles. In contrast, a similar amount of acid sites was present in catalysts containing over 7 wt% tungsten. Because a large gap was found in catalytic activity between the prepared catalysts, further studies will be required to identify additional influential factors. From FT-IR spectra of adsorbed NH_3, the compositions of acid type are clearly different. The fraction of Lewis acid sites to total acid sites increased from 23% to 77% as the increase in loading amount, due to the abundance of crystalline WO_3 which could be easily formed at high loading levels. From the quantitative study, the optimal level of Lewis acid sites in tungsten oxide for optimal esterification was 55%. This ratio contained the optimal levels of Lewis acid and Brønsted acid sites for attracting reactant and to function as the main active site, respectively, in the esterification reaction.

CONCLUSIONS

We examined tungsten oxide catalysts supported on silica for the esterification of acetic acid with ethanol, and identified the characteristics of the prepared catalysts, with the objective of defining the factors that influence the overall reaction. The number of acid sites is not the sole important factor as reported in the previous study and acid type present is also a crucial factor. Through a quantitative study, the optimum value for the portion of Lewis acid, around 55%, was found due to containing the optimal composition of Lewis

acid and Brønsted acid sites which, respectively, attract reactant to the catalyst and serve as main reaction sites.

ACKNOWLEDGEMENTS

This research is supported by Korea Ministry of Environment as "Converging technology project (202-101-009)". It was also supported by WCU (World Class University) program through the National Research Foundation of Korea funded by the Ministry of Education, Science and Technology (R31-10013).

REFERENCES

1. V. A. Coopman, J. A. Cordonnier and C. A. De Meyere, *Forensic Sci. Int.*, **154**, 92 (2005).
2. J. Wei, F. Li, H. Xing, S. Deng and Q. Ren, *Korean J. Chem. Eng.*, **26**, 666 (2009).
3. Y. J. Kim, S. D. Bhatt, S. Yoon, H. Y. Kim, Y. Lee and C. W. Lee, *Korean Chem. Eng. Res.*, **46**, 279 (2008).
4. S. K. Bhorodwaj, M. G. Pathak and D. K. Dutta, *Catal. Lett.*, **133**, 185 (2009).
5. F. Zhang, J. Wang, C. Yuan and X. Ren, *Catal. Lett.*, **102**, 171 (2005).
6. S. R. Kirumakki, N. Nagaraju and K. V. R. Chary, *Appl. Catal. A: Gen.*, **299**, 185 (2006).
7. S. Miao and B. H. Shanks, *J. Catal.*, **279**, 136 (2011).
8. W. Chu, X. Yang, X. Ye and Y. Wu, *Appl. Catal. A: Gen.*, **145**, 125 (1996).
9. C. Martin, P. Malet, G. Solana and V. Rives, *J. Phys. Chem. B*, **102**, 2759 (1998).
10. J. R. Sohn and J. H. Bae, *Korean J. Chem. Eng.*, **17**, 86 (2000).
11. G. Busca, *Phys. Chem. Chem. Phys.*, **1**, 723 (1999).
12. S. M. Kanan, Z. Lu and C. P. Tripp, *J. Phys. Chem. B*, **106**, 9576 (2002).
13. Y. Wang, Q. Chen, W. Yang, Z. Xie, W. Xu and D. Huang, *Appl. Catal. A: Gen.*, **250**, 25 (2003).
14. K. Wu and Y. Chen, *Appl. Catal. A: Gen.*, **257**, 33 (2004).
15. M. J. Verhoef, P. J. Kooyman, J. A. Peters and H. Bekkum, *Micropor. Mesopor. Mater.*, **27**, 365 (1999).
16. D. G. Barton, S. L. Soled and E. Iglesia, *Top. Catal.*, **6**, 87 (1998).
17. X. Xia, R. Jin, Y. He, J. Deng and H. Li, *Appl. Surf. Sci.*, **165**, 255 (2000).
18. A. Satsuma, K. Shimizu, T. Hattori, H. Nishiyama, S. Kakimoto, S. Sugaya and H. Yokoi, *Sensor Actuat. B: Chem.*, **123**, 757 (2007).
19. A. Spamer, T. I. Dube, D. J. Moodley, C. Schalkwyk and J. M. Botha, *Appl. Catal. A: Gen.*, **255**, 153 (2003).
20. C. Martýn, G. Solana, P. Malet and V. Rives, *Catal. Today*, **78**, 365 (2003).
21. A. Kuzmin, J. Purans, E. Cazzanelli, C. Vinegoni and G. Mariotto, *J. Appl. Phys.*, **84**, 5515 (1998).
22. P. Concepción, P. Botella and J. M. López Nieto, *Appl. Catal. A: Gen.*, **278**, 45 (2004).
23. J. M. G. Amores, V. S. Escribano, G. Ramis and G. Busca, *Appl. Catal. B: Environ.*, **13**, 45 (1997).
24. L. M. Cornaglia, E. A. Lombardo, J. A. Anderson and J. L. Gracia Fierro, *Appl. Catal.*, **100**, 37 (1993).
25. T. A. Peters, N. E. Benes, A. Holmen and Jos T. F. Keurentjes, *Appl. Catal. A: Gen.*, **297**, 182 (2006).
26. A. E. R. S. Khder, *Appl. Catal. A: Gen.*, **343**, 109 (2008).